Tetrahedron 66 (2010) 8512–8521

Contents lists available at ScienceDirect

Tetrahedron

journal homepage: www.elsevier.com/locate/tet

Tailor-made chiral pyranopyrans based on glucose and galactose and studies on self-assembly of some crystals and low molecular weight organogel (LMOG)

Soumik Roy [a], Arijit Chakraborty [a], Basab Chattopadhyay [b], Abir Bhattacharya [c], Alok K. Mukherjee [c], Rina Ghosh [a,*]

[a] Department of Chemistry, Jadavpur University, Raja S. C. Mallik Road, Kolkata, West Bengal 700032, India
[b] Department of Solid State Physics, Indian Association for the Cultivation of Science, Kolkata 700032, India
[c] Department of Physics, Jadavpur University, Kolkata 700032, India

ARTICLE INFO

Article history:
Received 9 July 2010
Received in revised form 19 August 2010
Accepted 23 August 2010
Available online 6 September 2010

Keywords:
Chiral pyranopyran
$InCl_3$
Organogelator
Organogel
Crystal assembly

ABSTRACT

$InCl_3$ catalyzed reactions of 2-*C*-acetoxymethylglycal derivatives with different phenolic compounds resulted in the formation of sugar based pyranoarenopyrans in good yields and moderate to excellent diastereoselectivity in favor of 10a*R*- or 12a*R*- or 14a*R*-products. One of the synthesized compounds, viz. (2*R*,3*R*,12a*R*)-2,3,5,12a-tetrahydro-2-methoxymethyl-3-methoxypyrano[2,3-*b*]naphtho[1,2-*e*]pyran gelated polar solvents like MeOH, EtOH and non-polar solvents like pentane, hexane, heptane, octane, pet. ether, etc. The SEM picture of the corresponding hexane xerogel exhibited a rare type of microtubular gel assembly, whereas the SEM pictures of MeOH and pet. ether xerogels showed different types of three-dimensional network. Study of the MeOH gel by Fluorescence spectroscopy, ^{1}H NMR and X-ray powder diffraction analysis indicated that the supramolecular assembly in the MeOH gel can be attributed to π-stacking. The crystal packing of (2*R*,3*R*,10a*R*)-3,10a-dihydro-2-methoxymethyl-3-methoxy-7-methyl-2*H*,5*H*-pyrano[2,3-*b*][1]benzopyran, a benzopyran analogue of the above organogelator was stabilized by C—H···O and C—H···π hydrogen bonds forming one-dimensional columns parallel to the [001] direction, whereas the corresponding benzopyran 3-epimer showed only C—H···O hydrogen bonds among the molecules.

1. Introduction

Low molecular mass organogelators and the corresponding gels are of current interest.[1] Gelators are capable of immobilizing various liquids creating novel superstructures of micro- or nanodimensions from supramolecular assembly, which are characterized by SEM and TEM. The functional properties of the gels having different superstructure can be studied by spectroscopic techniques and may be correlated with the aggregation mode. Gels of varied structures and functions may be utilized for different potential applications for light harvesting materials,[2a,b] solar cells,[2c] semiconductors,[2d,e] magneto-optical switches,[2f] sensorics,[2g] templates,[2h–j] sol–gel transcription,[2k] contact lense,[2l] plastic surgery,[2m] crystal engineering,[2n] etc. H-bonding, π-stacking, London dispersion forces, electrostatic interaction, etc. are the common driving forces for supramolecular assembly leading to gels[3] or crystals.[4]

Benzopyrans are potential oxygenated heterocycles occurring as the core structure of complex natural products.[5] Since the first synthesis of chiral pyrano[2,3-*b*]benzopyrans by reaction of 2-*C*-acetoxymethyl-D-glycal derivatives with phenols in the presence of $BF_3 \cdot Et_2O$,[6] there have been few other reports[7] including those from our laboratory[7b,c] on such syntheses. To the best of our knowledge, our preliminary report so far has been the only communication of organogel based on pyranoarenopyran.[7c] Synthesis of most of other benzopyrans is based on the condensation of salicylaldehyde or its derivatives with conjugated alkenes[8] or 3,4-dihydro-2*H*-pyrans.[9] In continuation to our preliminary communication on sugar derived chiral pyranopyrans[7b,c] and also as a part of our ongoing research programme on carbohydrate based organic syntheses,[7b,c,10] including organogelators and study of the corresponding gels,[10e] we report herein, the synthesis of some sugar modified new chiral pyranopyrans (Scheme 1, Table 1) along with the characterization of organogel from the chiral gelator (2*R*,3*R*,12a*R*)-2,3,5,12a-tetrahydro-2-methoxymethyl-3-methoxypyrano[2,3-*b*]naphtho[1,2-*e*]pyran [12a-(*R*)-**11**,[7c] Scheme 1] using electron microscopy, Fluorescence and ^{1}H NMR spectroscopy and X-ray diffraction studies. Crystal assembly of (2*R*,3*R*,10a*R*)-3,10a-dihydro-2-methoxymethyl-3-methoxy-7-methyl-2*H*,5*H*-pyrano[2,3-*b*][1]benzopyran [10a-(*R*)-**10**,[7b] a pyranobenzo pyran analogue of the above pyranonaphthopyran [12a-(*R*)-**11**], Scheme 1] has also been studied by X-ray powder diffraction.

* Corresponding author. Fax: +91 033 24146266; e-mail addresses: ghoshrina@yahoo.com, ghosh_rina@hotmail.com (R. Ghosh).

0040-4020/$ – see front matter © 2010 Elsevier Ltd. All rights reserved.
doi:10.1016/j.tet.2010.08.054

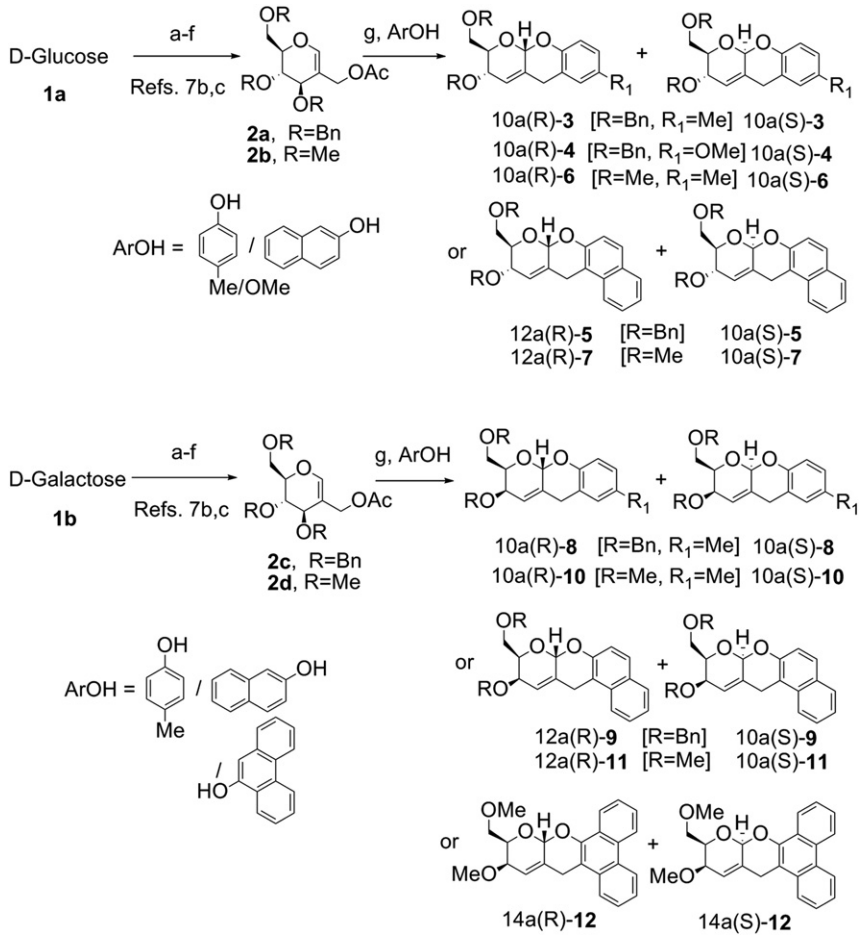

Scheme 1. Synthesis of glucose and galactose derived chiral pyranopyrans. Reagents and condition: (a) i. HBr/HOAc, Ac_2O; ii. Zn/Cu; (b) Et_3N/MeOH/H_2O; (c) NaH, DMF, RX; (d) $POCl_3$, DMF; (e) $NaBH_4$, MeOH; (f) Ac_2O, Py; (g) $InCl_3$ (cat.), CH_2Cl_2, amb. temp.

Table 1
$InCl_3$ catalyzed Ferrier rearrangement–tandem cyclisation of 2-acetoxyglycals towards synthesis of glucose and galactose derived chiral pyranopyrans

Entry	Substrate	Nucleophile	Time (h)	Product	% Yield[a] α[b]/Total yield	α/β
1	**2a**	*p*-Cresol	3.5	**3**	89/98	~10[c]
2	**2a**	*p*-Methoxy phenol	4	**4**	—/89	5[d]
3	**2a**	β-Naphthol	3	**5**	89/98	~10[c]
4	**2b**	*p*-Cresol	Overnight	**6**	—/84	2.5[d]
5	**2b**	β-Naphthol	6	**7**	81/89	~10[c]
6	**2c**	*p*-Cresol	3.5	**8**	—/83	>96% α[d]
7	**2c**	β-Naphthol	3	**9**	81/89	~10[c]
8	**2d**	*p*-Cresol	3	**10**	92/98	~15[c]
9	**2d**	β-Naphthol	6	**11**	61/83	2.5[d]
10	**2d**	9-Phenanthrol	3	**12**	81/83	~40[c]

[a] Chromatographed yield.
[b] Yield of α-glycosylated product.
[c] Based on isolated yields of pure isomers.
[d] Based on ^{1}H NMR.

2. Results and discussion

Glucose and galactose were converted to the corresponding 2-*C*-acetoxymethyl glycals (**2a**–**d**) following our earlier reported procedure.[7b,c] Indium chloride catalyzed reactions of (**2a**–**d**) with phenols or naphthols or 9-phenanthrol produce the corresponding pyranobenzo[2,3-*b*][1]pyrans (**3**, **4**, **6**, **8**, **10**), pyrano[2,3-*b*]naphtho[1,2-*e*]pyrans (**5**, **7**, **9**, **11**) or pyrano[2,3-*b*]phenanthro[9,10-*e*]pyrans (**12**) (Scheme 1) in very good yields (83–98%) and moderate to excellent diastereoselectivity (α:β 2.5 to ~40, Table 1). The reaction probably starts with initial exocyclic Ferrier rearrangement followed by tandem intramolecular cyclization via allylic nucleophilic displacement finally generating the pyranopyran; the probable mechanism and catalytic cycle are shown in Scheme 2. Both anomeric effect and stereochemistry of the hydroxyl groups on the glycal moiety contribute to the α-selectivity of the glycosidation step, and better α-selectivity is observed from D-galactose derived acetoxymethyl glycals (**2c** and **2d**).

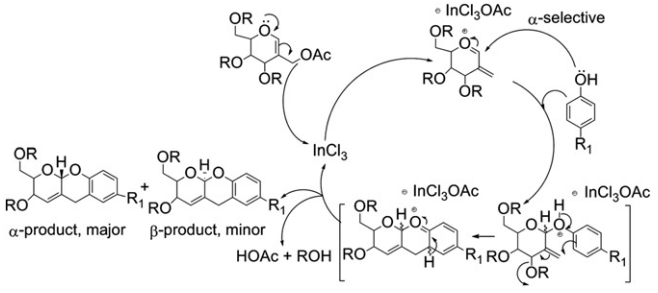

Scheme 2. Plausible mechanistic pathway and catalytic cycle of $InCl_3$ catalyzed chiral pyranopyran synthesis from 2-*C*-acetoxymethylglycal.

Among the synthesized compounds only (2*R*,3*R*,12a*R*)-2,3,5,12a-tetrahydro-2-methoxymethyl-3-methoxypyrano[2,3-*b*]naphtho[1,2-*e*]pyran [12a-(*R*)-**11**] gelated polar as well as non-polar solvents (Table 2), but its corresponding minor isomer [12a-(*S*)-**11**], which is epimeric with 12a-(*R*)-**11**, does not form gel. Compound 12a-(*R*)-**9** could neither be crystallized, nor could it gelate any solvent. All major products assembled into crystals (Table 2).

Table 2
Nature of assembly (crystal/gel) of compounds

Compound	Assembly	Solvent
10a-(*R*)-**3**	Crystal	Pet. ether, 60°–80 °C
10a-(*R*)-**4**	Crystal	Et_2O–pet. ether, 40°–60 °C
12a-(*R*)-**5**	Crystal	Pet. ether, 60°–80 °C
10a-(*R*)-**6**	Crystal	Pet. ether, 60°–80 °C
12a-(*R*)-**7**	Crystal	EtOAc–pet. ether, 60°–80 °C
10a-(*R*)-**8**	Crystal	Et_2O–pet. ether, 40°–60 °C
12a-(*R*)-**9**	Glassy material	Could not be crystallised
10a-(*R*)-**10**	Crystal	Pet. ether, 60°–80 °C, MeOH
12a-(*R*)-**11**	Gel	Hexane, heptane, octane, pet. ether; MeOH, EtOH
14a-(*R*)-**12**	Crystal	Pet. ether, 60°–80 °C

The results of gelation experiments of the gelator 12a(*R*)-**11** in different polar and non-polar solvents are given in Table 3, and the concentration dependent T_{gel} plots are depicted in Figure 1. 12a(*R*)-**11** Gelated alkanes like pentane, hexane, cyclohexane, heptane, octane and also polar protic solvents like methanol and ethanol. Except with cyclohexane, in all other cases thermo reversible gels were obtained, in cyclohexane a thixotropic unstable gel was formed. In general acyclic alkane gels were more shelf-stable than the corresponding alcohol gels. A slight gradual increase in the melting point of the alkane-gels was observed with increase in the alkyl chain length, whereas, MeOH gel had a greater T_{gel} than EtOH–gel (Fig. 1).

Table 3
Gelation test of the organogelator (12a-(*R*)-**11**) in different liquids

Entry	Organic solvent	12a-(*R*)-**11**	Minimum gelation concentration at 25 °C (mg/mL)/T_{gel}
1	Pet. ether (60–80 °C)	G	—
2	Pentane	G	12.0/41.0 °C
3	Hexane	G	10.9/43.0 °C
4	Heptane	G	10.0/44.0 °C
5	Octane	G	8.6/45.5 °C
6	Benzene	S	—
7	Toluene	S	—
8	Pyridine	S	—
9	Dichloromethane	S	—
10	Chloroform	S	—
11	Methanol	G	36.7/28.0 °C
12	Ethanol	G	48.8/28.5 °C
13	Isopropanol	S	—
14	Butanol	S	—
15	Cyclohexanol	S	—
16	Diethylether	S	—
17	Acetone	S	—
18	EtOAc–pet. ether (1:4)	OG	
19	Cyclohexane	TG	

G, gel. S, solution. OG, opaque gel. TG, thixotropic gel.

The morphology of the xerogels was studied by SEM experiments. The SEM picture of hexane xerogel exhibited a rare type of microtubular gel assembly,[7c] whereas MeOH xerogel (Fig. 2a) showed three-dimensional knitting structures, and pet. ether xerogel (Fig. 2b) showed fibrous network structures. It is interesting to note that almost similar 3D-network is initially formed in MeOH (Fig. 2a) and in hexane–gel, that in the later further generates microtubular structure (Fig. 2c).

Fluorescence spectroscopy of organogel–sol systems provides information on the supramolecular organization of the fluorophores in the gel.[11] The naphthalene moiety of the organogelator 12a-(*R*)-**11** would act as an intrinsic probe for characterization of its self-assembly behavior. Fluorescence emission depends on the aggregation morphology such as H-type or J-type assembly.[12] The fluorescence spectral changes at different concentrations of sols and gel in MeOH were taken by exciting at 334 and 280 nm (Fig. 3a and b), and those in hexane were measured by excitation at 280 nm (Fig. 3c). The peak at 375.04 nm with a shoulder peak at 418.26 nm (excitation at 334 nm, Fig. 3a) can be attributed to the presence of equilibrium between the gelator monomer (375.04 nm) with the corresponding dimmer or higher aggregate (415.06 nm) at dilute solution (2.1×10^{-2} M). In all of these fluorescence spectra, the intensity of the more prominent peak appearing at lower wavelength gradually diminishes with increase of the gelator concentration, and although, in the case of gelator–MeOH system, this peak ultimately vanishes at gel concentration (Fig. 3a), but, is still visible in the case of gelator–hexane system (Fig. 3c). In each of these cases, the intensity of the less prominent shoulder peak is gradually diminished and red shifted. Thus, in both of these systems, the gelator molecules aggregate by J-type assembly, and the gelator aggregation starts well ahead the gel concentration is achieved. Moreover, in the gelator–hexane gel, probably the gelator monomer still exists in equilibrium with gelator aggregates. The emission peaks at higher concentration of the gelator in sol and also in the gel states became broader and weaker than those in the initial dilute solutions, probably due to inner-filter effect.[13] Further information on the nature of excited state was obtained from nanosecond time resolved fluorescence decay experiments (exciting at 295 nm light) with the gelator solutions of 2.1×10^{-2} M, and 1.17×10^{-1} M concentrations in the sol as well as in the gel state (Fig. 3d). In each case, the fluorescence was found to decay with single component. Decay profiles showed short lifetime of 3.8 ns for the dilute solution and longer lifetimes of 5.05 ns and 5.43 ns for the sol at gel concentration and for the gel, respectively. This implies that aggregated structures are present in the sol state at gel concentration, which imposes some restrictions on the rotation and vibration of the groups of the molecule causing wide difference in decay time of the sol at gel concentration compared to that at dilute solution. A slight

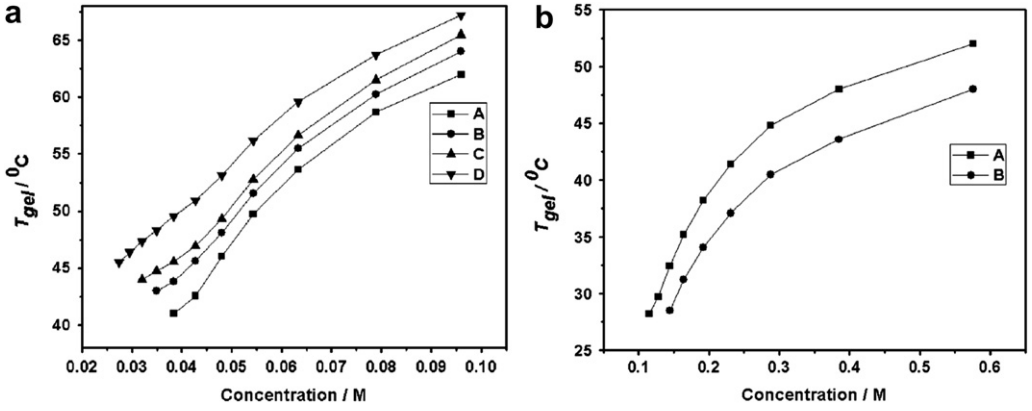

Fig. 1. Concentration dependence of the T_{gel} of 12a(*R*)-**11** gel (a) A: in pentane; B: in hexane; C: in heptane; D: in octane. (b) A: in MeOH; B: in EtOH.

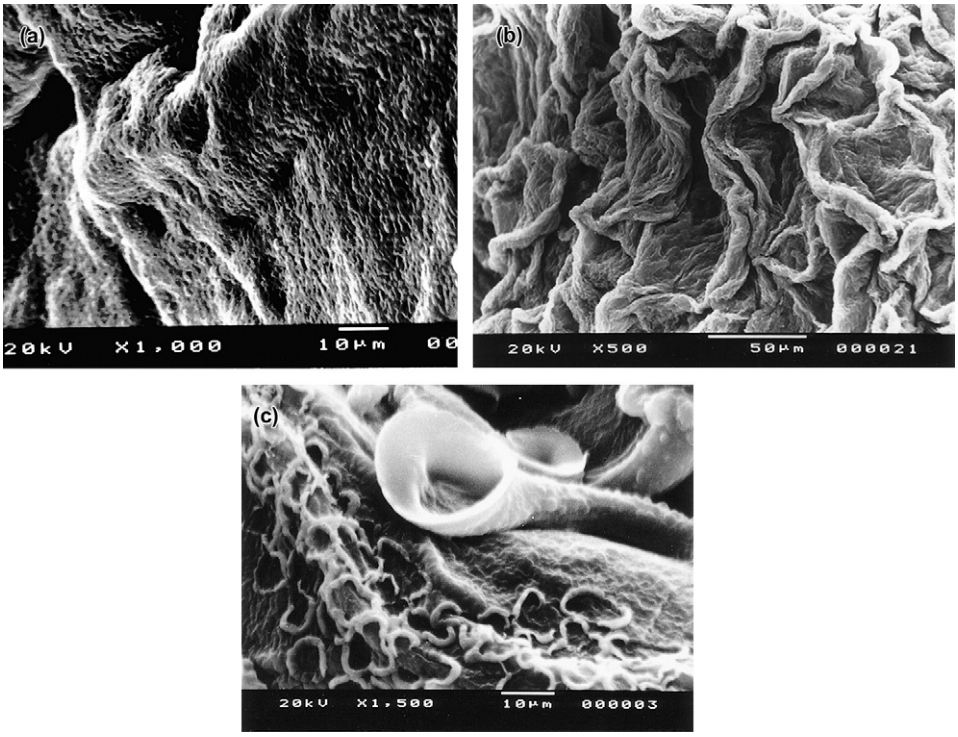

Fig. 2. SEM pictures of the xerogels of: (a) 12a-(*R*)-**11**–MeOH gel; (b)12a-(*R*)-**11**–pet. ether gel. (c) 12a-(*R*)-**11**–hexane (formation of microtubes from 3D-network is observed).

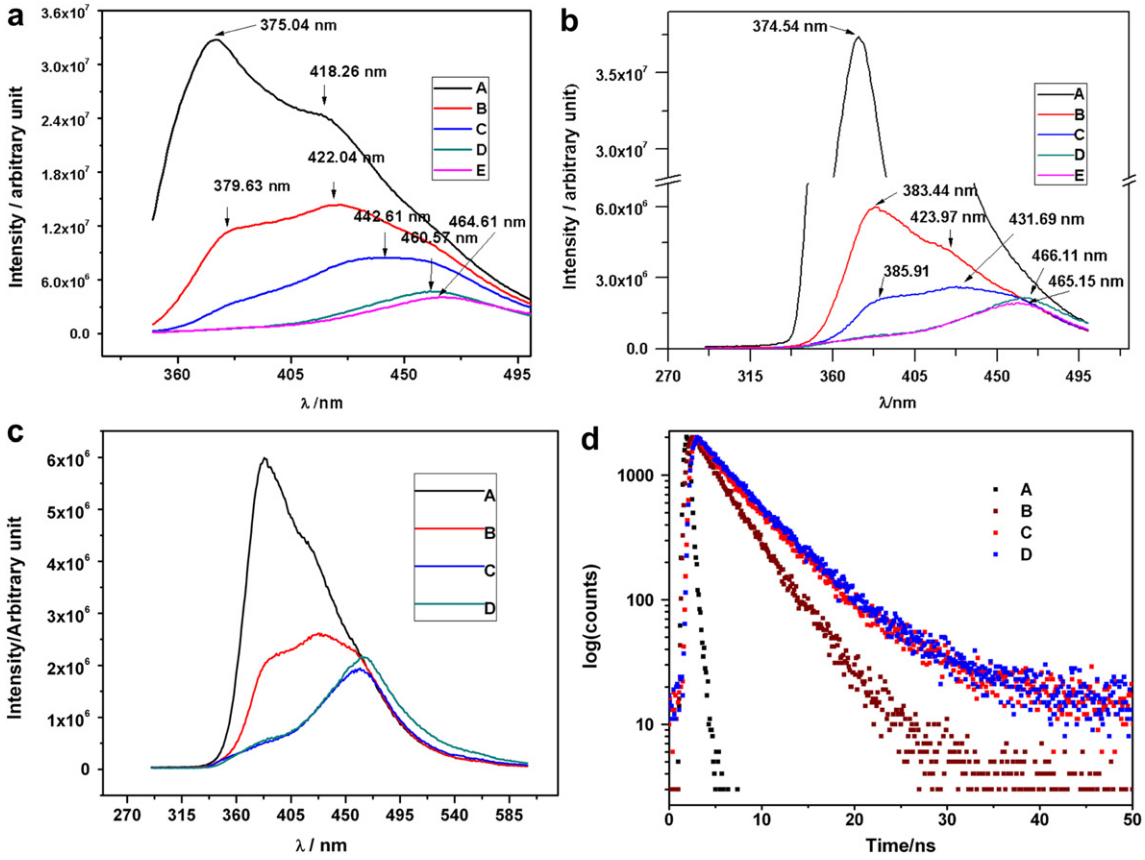

Fig. 3. Fluorescence emission spectra of 12a-(*R*)-**11** in methanol at different concentrations : (A) 2.1×10^{-2} M; (B) 4.8×10^{-2} M; (C) 6.9×10^{-2} M; (D) 1.17×10^{-1} M; (E) 1.17×10^{-1} M (gel) using (a) 334 nm and (b) 280 nm light as exiting source; (c) Fluorescence emission spectra of 12a-(*R*)-**11** in hexane at different concentrations: (A) 1.17×10^{-2} M; (B) 2.33×10^{-2} M; (C) 3.5×10^{-2} M; (D) 3.5×10^{-2} M (gel) using 280 nm light as exiting source; (d) Nanosecond time resolved Fluorescence decay of 12a-(*R*)-**11** in methanol at different concentrations : (A) prompt; (B) 2.1×10^{-2} M; (C) 1.17×10^{-1} M (sol); (D) 1.17×10^{-1} M (gel) using 295 nm nanoled as light source excitation.

longer decay time for the gel (5.43 ns) is detected, thus the gel is probably to some extent more structured with respect to its corresponding sol.

^{1}H NMR spectroscopy can provide valuable information about aggregation of gelators in the gel.[14] Thus, in order to get further information on the gel assembly ^{1}H NMR spectra of the gelator 12a-(*R*)-**11** in CD_3OD at different concentrations and temperature in the gel state (at 25 °C) and in solutions (at 25–40 °C, gel to sol transition temperature, T_{gel} ~29 °C) were recorded, which are presented in Figure 4. Interestingly, six proton-singlet at δ 3.45 ppm of 12a-(*R*)-**11** (monomer) at dilute concentration (2.1×10^{-2} M) representing two OMe protons, is split into two singlets at δ 3.45 and 3.43 ppm at a concentration of 6.9×10^{-2} M. At gel concentration (1.17×10^{-1} M) in the gel state this is further up-field shifted to δ 4.34 ppm. The fact that one 6H signal is observed at low concentration and two signals appear at higher concentrations may indicate increase of their non-equivalency due to constrains imposed by aggregation. Gradual up-field shifting of H_{2a} and $H_{2a'}$ and of one proton from the proton cluster corresponding to H_{5a}, H_{5a}, and H_3, is also observed upon changing the concentration from 6.9×10^{-2} M, sol to 1.17×10^{-1} M, gel. This is possible if the gelator molecules start aggregation even before gel concentration is achieved. This result is in accordance with the findings from Fluorescence experiments. The non-equivalence of two OMe protons is maintained in the gel as well as in the molten gel. Change in chemical shift as well as in the splitting pattern of the aromatic protons viz. H_6 and H_9 is also noticed at different concentrations of the gelator in the sol and gel states. Other proton signals, however, practically remain the same. Thus, one OMe, any one of H_5 or H_3 and H_6 and/or H_9 are somehow involved in the gelation process.

X-ray powder diffraction pattern of the gel compound 12a-(*R*)-**11** (Fig. 5) reveals a long-range periodic order with a low-angle peak at a *d*-spacing of 13.2 Å and two higher-order reflections at *d* values of 6.8 Å and 4.1 Å, respectively, corresponding to the ratio of 1:1/2:1/3. Furthermore, a prominent peak in the powder diffraction pattern characteristic of typical π–π stacking interaction was observed at *d*=3.7 Å (Fig. 5). The *d*-spacing of 5.5 Å can be

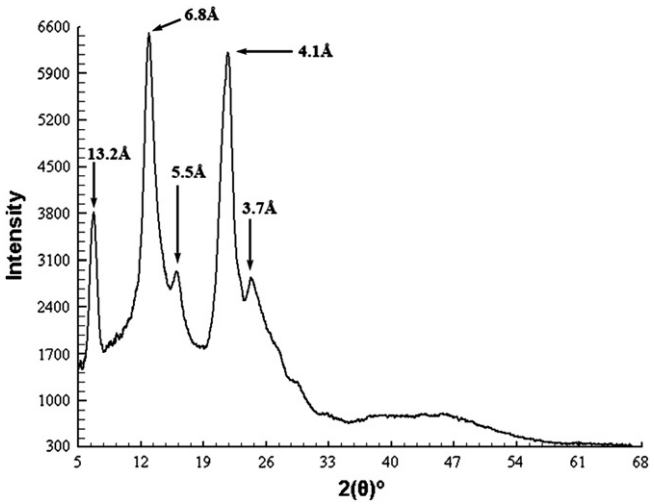

Fig. 5. X-ray powder diffraction pattern of the xerogel of MeOH-gelator [12a-(*R*)-**11**] system.

attributed to the separation between the columns formed by π–π stacking and side chain atom (C, O) interactions. Considering the approximate molecular length of 12a-(*R*)-**11**, 13.5 Å (Fig. 6a) as estimated by the DFT-calculations, it can be proposed that the molecules of 12a-(*R*)-**11** self-organize into a π-stacked lamellar (head to tail arrangement, as also evidenced from fluorescence red shift) assembly forming interdigitated bilayer structure with a thickness of 13.2 Å (Fig. 6b, b') giving tapes (Fig. 6c), which further assemble to form three-dimensional knitting ultimately resulting in gel network (Fig. 6d,e). Similar J-type aggregates have been reported for other gel compounds.[14b,15]

The Rietveld plot and the molecular view of 10a-(*R*)-**10** with atom-numbering scheme are shown in Figure. 7a and b, respectively. A summary of relevant crystal data of 10a-(*R*)-**10**,[16] the corresponding 3-epimer [10a-(*R*)-**6**][7b] and the napthopyranopyran analogue

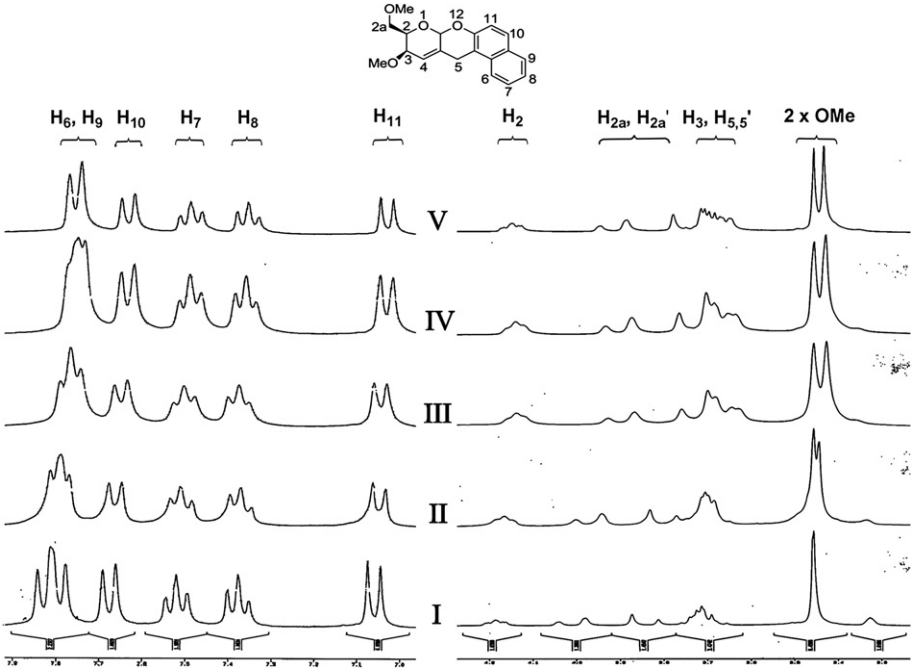

Fig. 4. ^{1}H NMR of 12a-(*R*)-**11** in CD_3OD at different concentrations: (I) 2.1×10^{-2} M; (II) 6.9×10^{-2} M; (III) 1.17×10^{-1} M (sol); (IV) 1.17×10^{-1} M (gel) at 25 °C and (V) 1.17×10^{-1} M (sol) at 30 °C.

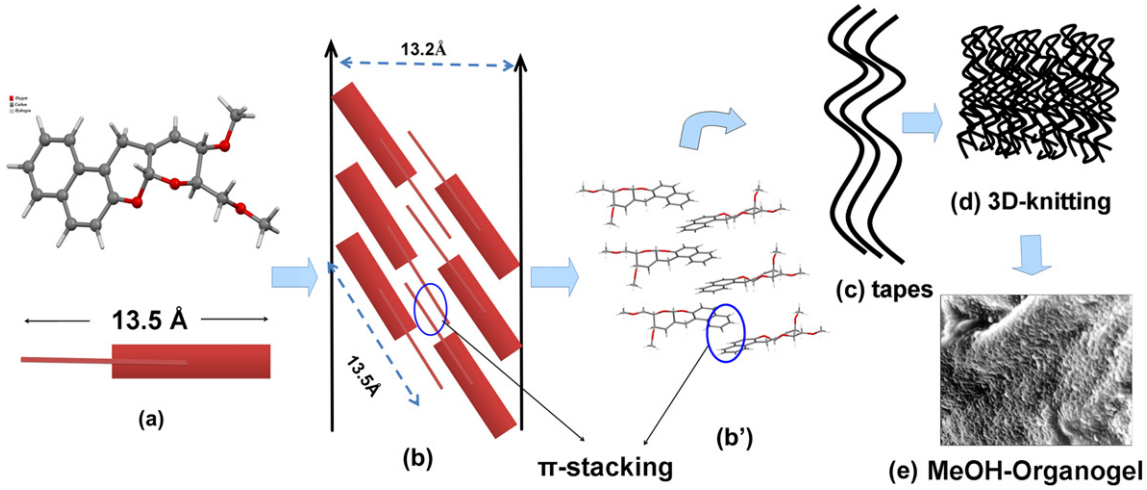

Fig. 6. Probable gelation mechanism: (a) DFT-based energy minimized model of gelator 12a-(*R*)-**11**; (b,b') Self-assembly of 12a-(*R*)-**11** forming bilayer structure through J-type aggregates generating tapes (c); (d) 3D-knitting of tapes; (e) MeOH–organogel.

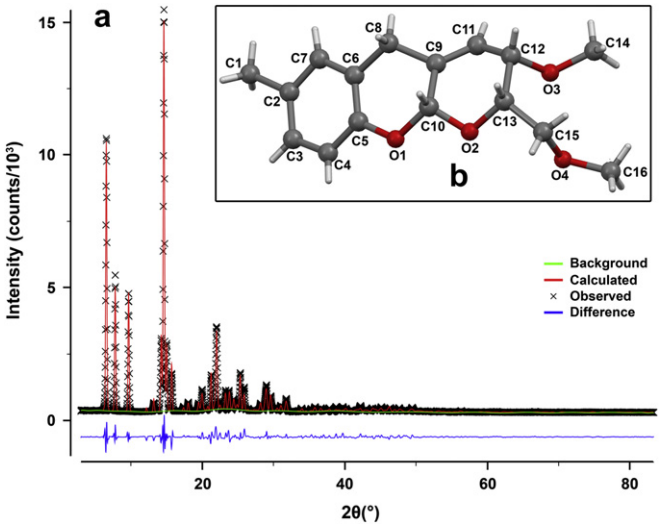

Fig. 7. (a). Final Rietveld plot for $C_{16}H_{20}O_4$ [10a-(*R*)-**10**]; (b). Inset: Molecular view of $C_{16}H_{20}O_4$ [10a-(*R*)-**10**].

12a-(*R*)-**7**[7c] of 10a-(*R*)-**10** is listed in Table 4. The molecule 10a-(*R*)-**10** consists of a fused benzopyrano-pyran moiety with the methoxy and methoxymethylene substitutions in one of the pyran rings and a methyl group in the peripheral aromatic ring. The conformation of pyranobenzopyran moiety in 10a-(*R*)-**10** (molecular length of 11.5 Å) as established from the present structure analysis using X-ray powder diffraction data is very similar to that of corresponding isomer [10a-(*R*)-**6**], the structure of which was established earlier from single-crystal X-ray analysis.[7b] Some significant differences in the relative orientation of substituted side chains in the pyran ring, however exist.

The crystal packing of 10a-(*R*)-**10** (Fig. 8a) and its epimer [10a-(*R*)-**6**] (Fig. 8b) exhibits similar type of stacking of molecules along the shortest crystal axis with interlayer separations of 4.5 Å in both of 10a-(*R*)-**10** and 10a-(*R*)-**6**. In 10a-(*R*)-**10**, a combination of C–H···O and C–H···π hydrogen bonds, C15-HB (C15)···O3 [C15···O3 3.198 (7) Å, C15-HB (C15)···O3 140°] and C10-H10···C_g(C2–C7) [C10···C_g 3.084 (6) Å], connects the molecules into one-dimensional columns parallel to the [001] direction (Fig. 8a, inset). A similar one-dimensional columnar packing in [10a-(*R*)-**6**] is achieved through intermolecular C–H···O hydrogen bonds [C···O 3.561 (1) Å, C–H···O 153°] (Fig. 8b, inset).

Table 4
Crystal data for $C_{16}H_{20}O_4$ [10a-(*R*)-**10**], the corresponding 3-epimer [10a-(*R*)-**6**] and its naphthopyrano-pyran analogue [12a-(*R*)-**7**]

	$C_{16}H_{20}O_4$ [10a-(*R*)-**10**][16]	$C_{16}H_{20}O_4$ [10a-(*R*)-**6**][7b]	$C_{19}H_{20}O_4$ [12a-(*R*)-**7**][7c]
Formula weight	276.32	276.32	312.35
Temperature	293 (2) K	293 (2) K	293 (2) K
Structure analysis	Powder diffraction	Single-crystal diffraction	Single-crystal diffraction
Crystal system	Orthorhombic	Monoclinic	Orthorhombic
Space group	$P2_12_12_1$	$P2_1$	$P2_12_12_1$
Z	4	2	4
Unit cell dimensions	*a*=26.486 (3) Å	*a*=11.059 (2) Å	*a*=4.585 (1) Å
	b=12.2935 (4) Å	*b*=4.484 (1) Å	*b*=11.149 (1) Å
	c=4.4605 (2) Å	*c*=15.342 (3) Å	*c*=30.445 (4) Å
		β=107.941 (4)°	
Volume	1452.4 (2) Å^3	723.7 (2) Å^3	1556.2 (3) Å^3
2*θ* interval (°)	3–85°	2.8–44.98°	3.9–50°
Wavelength (Å)	1.54056	0.71073	0.71073
R_p/*R*1	0.0506	0.0741	0.0453
R_{wp}/*wR*	0.0723	0.1115	0.0958
$R(F^2)$	0.169		
χ^2/GOF	3.94	1.157	0.978

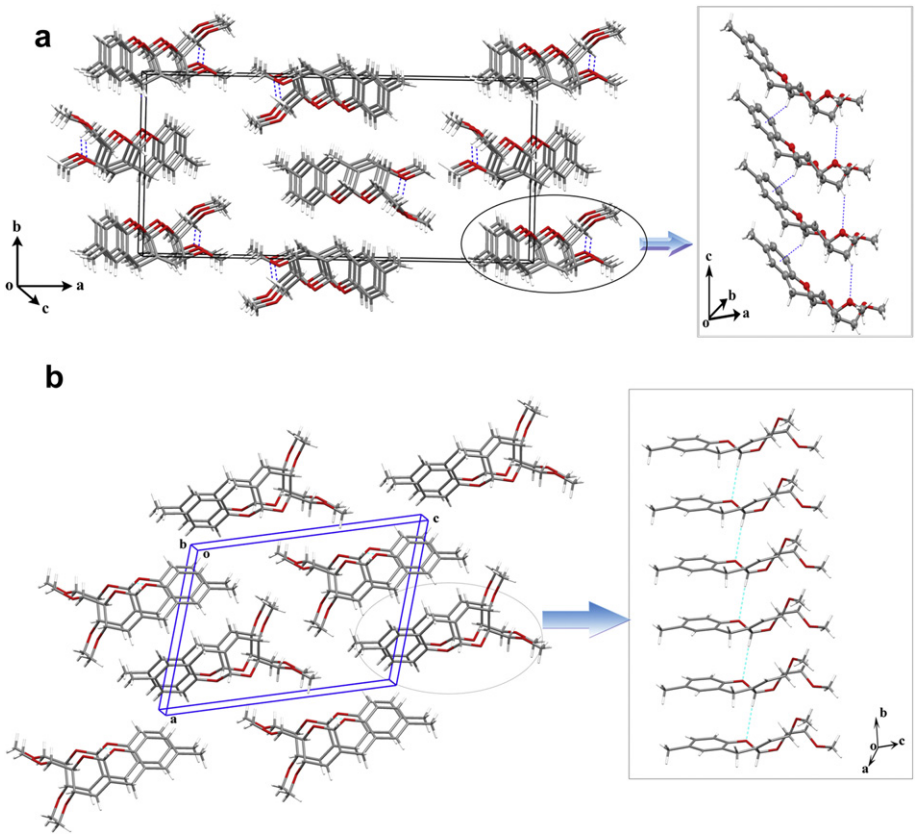

Fig. 8. a). Crystal packing of $C_{16}H_{20}O_4$ [10a-(*R*)-**10**][16] viewed down *c*-axis. Inset showing the infinite one-dimensional chain formed by C–H···O and C–H···π hydrogen bonds. b). Crystal packing of $C_{16}H_{20}O_4$ [10a-(*R*)-**6**] as reported by Ghosh et al.[7b] Inset showing the infinite one-dimensional chain formed by C–H···O hydrogen bonds.

3. Conclusion

In summary, several glucose and galactase derived chiral pyranoarenopyrans have been synthesized. The crucial step of the synthesis is $InCl_3$ catalyzed Ferrier rearrangement followed by tandem cyclization of 2-*C*-acetoxymethylglycal derivatives, which proceeds in excellent yields and moderate to excellent diastereoselectivities. Among the synthesized compounds the galactose based methoxylated pyrano[2,3-*b*]naphtho[1,2-*e*]pyran only formed organogel in polar as well as in non-polar solvents. Spectroscopic studies (Fluorescence and ^{1}H NMR) along with XRPD indicated that organogelator molecules initially self-organize in MeOH into a π-stacked lamellar assembly with J-type aggregates forming tapes, which finally assemble to give three-dimensional gel network. Crystal assembly of (2*R*,3*R*,10a*R*)-3,10a-dihydro-2-methoxymethyl-3-methoxy-7-methyl-2*H*,5*H*-pyrano[2,3-*b*][1]benzopyran, a benzopyran analogue of the gelator, was studied by XRPD, which showed C–H···O and C–H···π hydrogen bonds connecting the molecules into one-dimensional columns parallel to the [001] direction; whereas crystal assembly of the 3-epimer of the latter showed only C–H···O type hydrogen bond among connecting molecules as revealed by its XRD.

4. Experimental

4.1. Materials and instrumentation

Column chromatography was done on silica gel (60–120 mesh and 230–400 mesh). All solvents were dried and/or distilled (as required) before use. 9-Phenanthrol was purchased from Sigma–Aldrich. All other reagents and solvents were purchased from SRL, India. Melting points were observed on Toshniwal melting point apparatus and are uncorrected. Optical rotations were observed on Jasco J-815 spectrometer. IR spectra were recorded in a Perkin–Elmer Spectrum 100 FTIR spectrometer. UV spectra were taken on UV 1601 Shimadzu spectrophotometer. ^{1}H and ^{13}C NMR were recorded on Bruker DPX-300 NMR spectrometer operating at 300 MHz and 75 MHz for ^{1}H and ^{13}C NMR, respectively. All the high resolution mass spectrometric (HRMS) data were acquired on a Qtof Micro quadruple mass spectrometer using negative ionization method from HRMS laboratory at IACS, Kolkata 700 032, India. In all cases where the spectra of gels were recorded the gel was formed by cooling the corresponding sol at gel concentration in the UV cell or in the NMR tube. SEM pictures of the xerogels were taken in JEOL ISN 5200 scanning microscope. Fluorescence emissions were observed in SPEX FlUOROLOG spectrophotometer. Fluorescence decays were observed using IBH, UK nanoLED applying 295 nm as the source light and the data were analyzed in IBH DH6 software.

4.2. General procedure

In general pyranopyrans were synthesized following the method described in our earlier communication.[7c] A detailed synthetic route to these compounds is shown in Scheme 1.

4.2.1. Preparation of sugar derived pyranopyran from 2-C-acetoxymethylglycal. To a mixture of 2-*C*-acetoxymethylglycal (100 mg), dry CH_2Cl_2 (5 mL) and molecular sieves (4 Å), phenol (1.2 equiv) was added and stirred magnetically in an ice-bath for 15 min $InCl_3$ (30 mol %) was then added to the reaction mixture under cold condition (0–5 °C) and the reaction mixture was allowed to come

to the room temperature. After the completion of the reaction (3 h—overnight, Table 1, checked by TLC using 3:1 pet. ether/ethyl acetate on silica gel) the reaction mixture was filtered through a Celite bed over 4% NaOH solution (15 mL) and the bed was washed with CH_2Cl_2 (3×10 mL). The organic layer of the combined filtrate and washings was washed with water (2×10 mL). The organic layer was dried over anhydrous Na_2SO_4 and then evaporated under reduced pressure to afford the crude pyranopyran. The crude product was purified by column chromatography on silica gel (60–120 mesh or 230–400 mesh) using benzene/ether solution as mobile phase.

*4.2.1.1. (2R, 3S, 10aR)-3,10a-Dihydro-2-benzyloxymethyl-3-benzyloxy-7-methyl-2H,5H-pyrano[2,3-b][1]benzopyran [10a-(R)-**3**]*[7d]. Yield: 89%; white crystal; mp 85 °C (from pet. ether 60–80 °C) (lit.,[7d] 85 °C); R_f (6% benzene/diethyl ether) 0.77; $[\alpha]_D^{25}$ −83.3 (*c* 0.9, $CHCl_3$) (lit.,[7d] −81); λ_{max} ($CHCl_3$) (log ε) 284.58 (3.44), 274.80 (3.42), 244.22 (3.26) nm; ν_{max} (KBr plate) 3040, 2864, 1605, 1590, 1495, 1390, 1310, 1200, 1170, 1120, 1075, 960, 930 cm^{-1}; δ_H (300 MHz, $CDCl_3$) 7.37–7.22 (10H, m), 6.89 (1H, d, *J* 8.1 Hz), 6.82–6.76 (2H, m), 5.98 (1H, s), 5.51 (1H, s), 4.69–4.45 (4H, m), 4.38 (1H, dd, *J* 8.9 Hz, 3.1 Hz), 3.94–3.91 (1H, m), 3.80 (2H, d, *J* 2.4 Hz), 3.68 (1H, d, *J* 17.5 Hz), 3.33 (1H, d, *J* 17.7 Hz), 2.23 (3H, s); δ_C (75 MHz, $CDCl_3$) 151.39, 138.09, 137.90, 130.52, 130.35, 128.91, 128.39, 128.23, 127.97, 127.86, 127.80, 127.66, 123.75, 120.60, 116.96, 93.68, 73.55, 71.90, 71.39, 70.38, 68.23, 32.97, 20.47; HRMS: $[M+Na]^+$, found 451.1880. $C_{28}H_{28}O_4Na$ requires 451.1885.

*4.2.1.2. (2R, 3S, 10aR)-3,10a-Dihydro-2-benzyloxymethyl-3-benzyloxy-7-methoxy-2H,5H-pyrano[2,3-b][1]benzopyran [10a-(R)-**4**]*[6,7d]. Yield: 75%; white crystal; mp 103–104 °C (from ether/pet. ether 40–60 °C) (lit.,[7d] 102–103 °C); R_f (6% benzene/diethyl ether) 0.68; $[\alpha]_D^{25}$ −85.2 (*c* 0.9, $CHCl_3$) (lit.,[7d] −83); λ_{max} ($CHCl_3$) (log ε) 290.33 (3.62), 252.12 (3.28), 280.22 (3.45) nm; ν_{max} (KBr plate) 3040, 2866, 1605, 1590, 1495, 1390, 1310, 1200, 1170, 1120, 1075, 960, 930 cm^{-1}; δ_H (300 MHz, $CDCl_3$) 7.60–7.23 (10H, m), 6.81 (1H, d, *J* 8.8 Hz), 6.66–6.70 (1H, dd, *J* 8.8 Hz, 2.6 Hz), 6.56 (1H, s), 5.99 (1H, s), 5.50 (1H, s), 4.69–4.46 (4H, m), 3.96–3.93 (2H, m), 3.81–3.68 (6H, m), 3.33–3.39 (1H, d, *J* 17.8 Hz); δ_C (75 MHz, $CDCl_3$) 153.90, 147.56, 138.05, 137.88, 130.41, 129.35, 128.37, 127.96, 127.88, 127.83, 127.68, 123.89, 121.53, 117.83, 116.02, 114.76, 113.64, 113.10, 93.64, 73.56, 71.92, 71.42, 70.37, 68.19, 55.71, 33.20; HRMS: $[M+Na]^+$, found 467.1832. $C_{28}H_{28}O_5Na$ requires 467.1834.

*4.2.1.3. (2R, 3S, 12aR)-2,3,5,12a-Tetrahydro-2-benzyloxymethyl-3-benzyloxypyrano[2,3-b]naphtho[1,2-e]pyran [12a-(R)-**5**]*[7d]. Yield: 89%; white crystal; mp 167–168 °C (from pet. ether) (lit.,[7d] 164–165 °C); R_f (6% benzene/diethyl ether) 0.85; $[\alpha]_D^{25}$ −207 (*c* 0.7, $CHCl_3$) (lit.,[7d] $[\alpha]_D^{25}$ −206.6); λ_{max} ($CHCl_3$) (log ε) 336.35 (3.32), 282.44 (4.54), 252.80 (3.36) nm; ν_{max} (KBr plate) 3030, 2902, 1596, 1465, 1391, 1363, 1230, 1176, 1073, 971 cm^{-1}; δ_H (300 MHz, $CDCl_3$) 7.76 (2H, dd, *J* 11.7 Hz, 8.6 Hz), 7.65 (1H, d, *J* 8.9 Hz), 7.50 (1H, t, *J* 7.4 Hz), 7.38–7.26 (11H, m), 7.13–7.10 (1H, d, *J* 8.9 Hz), 6.12 (1H, s), 5.64 (1H, s), 4.72–4.49 (4H, m), 4.41–4.40 (1H, d, *J* 6.8 Hz), 4.04–4.00 (1H, d, *J* 9.0 Hz), 3.93 (1H, d, *J* 18.2 Hz), 3.86 (2H, m), 3.77 (1H, d, *J* 17.5 Hz); δ_C (75 MHz, $CDCl_3$) 151.24, 138.10, 137.89, 132.19, 130.39, 129.20, 128.49, 128.41, 127.97, 127.89, 127.68, 126.65, 124.31, 123.69, 121.84, 119.00, 112.78, 93.71, 73.58, 72.14, 71.45, 70.49, 68.29, 30.39; HRMS: $[M+Na]^+$, found 487.1880. $C_{31}H_{28}O_4Na$ requires 487.1885.

*4.2.1.4. (2R, 3S, 12aS)-2,3,5,12a-Tetrahydro-2-benzyloxymethyl-3-benzyloxypyrano[2,3-b]naphtho[1,2-e]pyran [12a-(S)-**5**].* Glassy solid(uncrystallised); yield: 9%; mp 118 °C; R_f (6% benzene/diethyl ether) 0.83; $[\alpha]_D^{25}$ 107 (*c* 0.7, $CHCl_3$); λ_{max} ($CHCl_3$) (log ε) 338.70 (3.30), 281.46 (4.27), 251.73 (3.68) nm; ν_{max} (KBr plate) 3030, 2982, 2930, 2820, 1835, 1596, 1465 cm^{-1}; δ_H (300 MHz, $CDCl_3$) 7.79–7.73 (2H, m), 7.67–7.64 (1H, d, *J* 8.9 Hz), 7.51 (1H, t, *J* 7.5 Hz), 7.40–7.23 (11H, m), 7.13–7.10 (1H, d, *J* 8.9 Hz), 6.12 (1H, s), 5.74 (1H, s), 4.67–4.60 (2H, m), 4.58–4.53 (2H, m), 4.29–4.23 (1H, dd, *J* 10.2 Hz, 5.2 Hz), 4.13 (1H, br, s), 3.97–3.90 (1H, d, *J* 18.8 Hz), 3.80–3.73 (2H, m), 3.69–3.65 (1H, m); HRMS: $[M+Na]^+$, found 487.1882. $C_{31}H_{28}O_4Na$: requires 487.1885.

*4.2.1.5. (2R, 3R, 10aR)-3,10a-Dihydro-2-benzyloxymethyl-3-benzyloxy-7-methyl-2H,5H-pyrano[2,3-b][1]benzopyran [10a-(R)-**8**]*[7d]. Yield: 81%; white crystal; mp 98–99 °C (from ether/pet. ether 40–60 °C) (lit.,[7d] 99–100 °C); R_f (6% benzene/diethyl ether) 0.72; $[\alpha]_D^{25}$ −265 (*c* 0.8, $CHCl_3$) (lit.,[7d] $[\alpha]_b^{25}$ −268); λ_{max} ($CHCl_3$) (log ε) 282.66 (3.66), 257.91 (4.88), 246.30 (3.32) nm; ν_{max} (KBr plate) 3040, 2886, 1600, 1588, 1485 cm^{-1}; δ_H (300 MHz, $CDCl_3$) 7.37–7.26 (10H, m), 6.93 (1H, d, *J* 8.0 Hz), 6.85–6.79 (2H, m), 6.08 (1H, d, *J* 4.3 Hz), 5.60 (1H, s), 4.68 (2H, d, *J* 11.9 Hz), 4.59 (2H, d, *J* 11.9 Hz), 4.27–4.22 (1H, m), 3.89–3.84 (3H, m), 3.75 (1H, d, *J* 17.6 Hz), 3.35 (1H, d, *J* 17.8 Hz), 2.25 (3H, s); δ_C (75 MHz, $CDCl_3$) 151.39, 138.09, 137.90, 130.52, 130.35, 128.91, 128.39, 128.23, 127.97, 127.86, 127.80, 123.65, 120.60, 116.96, 93.68, 73.55, 71.89, 71.39, 70.38, 68.23, 32.97, 20.47; HRMS: $[M+Na]^+$, found 451.1882. $C_{28}H_{28}O_4Na$ requires 451.1885.

*4.2.1.6. (2R, 3R, 12aR)-2,3,5,12a-Tetrahydro-2-benzyloxymethyl-3-benzyloxypyrano[2,3-b]naphtho[1,2-e]pyran [12a-(R)-**9**]*[7d]. Yield: 81%; faint yellow syrup; R_f (6% benzene/diethyl ether) 0.81; $[\alpha]_D^{25}$ −256 (*c* 0.9, $CHCl_3$) (lit.,[7d] −254.89); λ_{max} ($CHCl_3$) (log ε) 337.10 (3.47), 287.32 (4.33), 254.80 (3.36) nm; ν_{max} (neat) 3067, 3018, 2855, 1598, 1466, 1397 cm^{-1}; δ_H (300 MHz, $CDCl_3$) 7.76 (1H, dd, *J* 11.5 Hz, 8.7 Hz), 7.65 (1H, d, *J* 8.9 Hz), 7.53–7.48 (1H, m), 7.40–7.26 (11H, m), 7.15–7.14 (2H, d, *J* 9.0 Hz), 6.22–6.20 (1H, m), 5.72 (1H, s), 4.74–4. 59 (4H, m), 4.34–4.30 (1H, m), 3.98 (1H, d, *J* 17.8 Hz), 3.90–3.88 (3H, m), 3.77 (1H, d, *J* 18.1 Hz); δ_C (75 MHz; $CDCl_3$) 151.16, 138.30, 138.08, 134.58, 132.18, 129.21, 128.52, 128.40, 127.85, 127.78, 127.68, 126.69, 123.75, 121.81, 120.31, 119.01, 112.77, 93.55, 73.56, 71.85, 71.28, 68.87, 67.59, 30.89; HRMS: $[M+Na]^+$, found 487.1883. $C_{31}H_{28}O_4Na$ requires 487.1885.

*4.2.1.7. (2R, 3R, 12aS)-2,3,5,12a-Tetrahydro-2-benzyloxymethyl-3-benzyloxypyrano[2,3-b]naphtho[1,2-e]pyran [12a-(S)-**9**].* Yield: 8%; faint yellow solid (uncrystallised); mp 120 °C; R_f (6% benzene/diethyl ether) 0.79; $[\alpha]_D^{25}$+111.2 (*c* 0.4, $CHCl_3$); λ_{max} ($CHCl_3$) (log ε) 338.75 (3.64), 282.74 (4.88), 245.57 (3.32) nm; δ_H (300 MHz, $CDCl_3$) 7.80–7.73 (2H, m), 7.68–7.65 (1H, d, *J* 8.9 Hz), 7.54–7.49 (1H, t, *J* 7.6 Hz,), 7.41–7.29 (10H, m), 7.19–7.15 (1H, d, *J* 8.9 Hz), 6.13 (1H, s), 5.74 (1H, s), 4.70–4.59 (4H, m), 4.24–4.19 (4H, m), 4.19 (1H, br, s), 3.90–3.75 (4H, m); δ_C (75 MHz, $CDCl_3$) 149.86, 138.33, 138.10, 134.11, 131.90, 129.39, 128.58, 128.39, 128.37, 128.33, 127.90, 127.78, 127.68, 127.64, 126.66, 123.82, 122.17, 121.76, 118.84, 112.43, 94.69, 74.53, 73.71, 70.79, 69.15, 69.07, 28.45; HRMS: $[M+Na]^+$, found 487.1884. $C_{31}H_{28}O_4Na$: requires 487.1885.

*4.2.1.8. (2R, 3R, 10aR)-3,10a-Dihydro-2-methoxymethyl-3-methoxy-7-methyl-2H,5H-pyrano[2,3-b][1]benzopyran [10a-(R)-**10**]*[7d]. Yield: 92%; faint yellow solid; mp 85 °C (from MeOH) (lit.,[7d] 84–86 °C); R_f (6% benzene/diethyl ether) 0.60; $[\alpha]_D^{25}$ −176.4 (*c* 0.9, $CHCl_3$); (lit.,[7d] −175.2); λ_{max} ($CHCl_3$) (log ε) 240.56 (3.25), 284.58 (3.39) nm; ν_{max} (KBr plate) 2910, 2886, 1578, 1490, 1450, 1380, cm^{-1}; δ_H (300 MHz, $CDCl_3$) 6.94 (1H, d, *J* 8.1 Hz), 6.80–6.79 (2H, m), 6.20–6.17 (1H, dd, *J* 5.8 Hz, 2.1 Hz), 5.58 (1H, s), 4.20–4.15 (1H, m), 3.79–3.69 (3H, m), 3.64–3.62 (1H, m), 3.45 (3H, s), 3.43 (3H, s), 3.40–3.34 (1H, d, *J* 18.1 Hz), 2.25 (3H, s); δ_C (75 MHz, $CDCl_3$) 151.31, 135.12, 130.43, 128.87, 128.28, 120.54, 119.17, 117.06, 93.38, 71.44, 69.63, 59.24, 53.34, 33.51, 20.39; HRMS: $[M+Na]^+$, found 299.1261.$C_{16}H_{20}O_4Na$ requires 299.1259.

*4.2.1.9. (2R, 3R, 14aR)-2,3,5,14a-Tetrahydro-2-methoxymethyl-3-methoxypyrano[2,3-b]phenanthreno[9,10-e]pyran [14a-(R)-**12**].* Yield: 81%; faint yellow crystal; mp 128 °C (from pet. ether); R_f (6% benzene/diethyl ether) 0.75; $[\alpha]_D^{25}$ −269.2 (*c* 0.9, $CHCl_3$); λ_{max} ($CHCl_3$) (log ε) 248.92 (3.30), 298.56 (4.73), 354.85 (3.85), 380.12 (3.45) nm; ν_{max} (KBr plate) 3030, 2902, 1596, 1475, cm^{-1}; δ_H (300 MHz, $CDCl_3$) 8.63 (1H, d, *J* 7.2 Hz), 8.62 (1H, d, *J* 7.0 Hz), 8.40 (1H, d, *J* 8.9 Hz), 7.79 (1H, d, *J* 7.7 Hz), 7.67–7.56 (4H, m), 6.36 (1H, d, *J* 3.9 Hz), 5.84 (1H, s), 4.37–4.32 (1H, m), 4.04 (1H, d, *J* 18.0 Hz), 3.86–3.80 (2H, m), 3.77 (1H, d, *J* 5.0 Hz), 3.71 (1H, dd, *J* 5.7 Hz, 1.8 Hz), 3.52 (3H, s), 3.49 (3H, s); δ_C (75 MHz, $CDCl_3$) 155.16, 136.25, 134.75, 132.12, 129.08, 126.90, 126.85, 123.75, 122.70, 121.42, 121.37, 120.00, 112.60, 93.56, 71.73, 71.54, 69.65, 59.31, 56.86, 30.90; HRMS: $[M+Na]^+$, found 385.1412. $C_{23}H_{22}O_4Na$ requires 385.1416.

4.3. Gelation test and determination of T_{gel}

In a typical procedure 0.012 g of the compound 12a-(*R*)-**11** was taken in a vial and 0.4 mL of hexane was added and the cap of the vial was closed tightly. It was warmed carefully in a water bath and the vial containing the clear solution was cooled immediately in an ice-bath to check gel formation. If the jelly matter remained intact at 25 °C even in an inverted position of the vial, it was supposed to be a gel. To determine the T_{gel} the tightly capped vial containing the gel was heated slowly in a water bath and the temperature at which the gel swelled thoroughly was noted as the T_{gel} for the respective concentration. Now 0.1 mL of hexane was added again, and the T_{gel} for that concentration was determined similarly. Addition of hexane was continued till the dilution reached where the whole of the hexane was not gelated at 25 °C.

4.4. X-ray powder diffraction analysis

X-ray powder diffraction data of 10a-(*R*)-**10** and 12a-(*R*)-**11** were collected on a Bruker D8 Advance powder diffractometer using monochromatic CuKα_1 radiation (λ=1.54056 Å) selected with an incident beam germanium monochromator. The diffraction patterns were recorded at 25 °C with a step size of 0.02°, and counting time 20 s/step over an angular range (2θ) 3–85° for 10a-(*R*)-**10**, and counting time of 25s/step and an angular range (2θ) 5–65° for 12a-(*R*)-**11**, using the Bragg-Brentano geometry. The diffraction pattern of 10a-(*R*)-**10** was indexed using the program NTREOR,[17] to an orthorhombic cell with *a*=26.5998 (8) Å, *b*=12.3414 (8) Å, *c*=4.4796 (9) Å and *V*=1470.6 $Å^3$ [M_{20}=29, F_{20}=75]. Statistical analysis of the powder diffraction data of 10a-(*R*)-**10** indicated $P2_12_12_1$ as the most probable space group, which was used for structure analysis. The structure of 10a-(*R*)-**10** was solved ab initio by global optimization of a structural model in direct space using the program FOX.[18] The initial molecular geometry used in FOX was optimized from MOPAC 2009.[19] Lattice and profile parameters, zero-point and interpolated background calculated from a previous powder-pattern decomposition based on the Le Bail algorithm, were introduced into the program FOX, while keeping the bond lengths and bond angles constrained within 0.10 Å and 5.0°, respectively. The best trial structure (R_{wp}=0.0848) obtained from the parallel tempering procedure of FOX was used as the starting model for Rietveld refinement using the program GSAS.[20] In the Rietveld refinement, standard restraints were applied on the bond lengths and bond angles; hydrogen atoms were placed at the calculated positions towards the final stages of refinement. The final refinement (Fig. 7a) converged to R_{wp}=0.0723, R_p=0.0506, $R(F^2)$=0.169 and χ^2=3.94.

Acknowledgements

The authors are grateful to DST, New Delhi, India for funding of project (No. SR/S1/OC-28/2006) to R.G., and to UGC, India for supporting fellowship (SRF) to S.R. Professor N. Chattopadhyay, Department of Chemistry, Jadavpur University is warmly thanked for providing Fluorescence spectroscopic facilities. Supports from CAS-UGC, India and FIST-DST, India to the Department of Chemistry, Jadavpur University, Kolkata are also acknowledged.

Supplementary data

Electronic Supplementary Information (ESI) available: Spectra (^1H and ^{13}C NMR) of compounds 10a- (*R*)-**3**, **-4**, **-8**, **-10**; 12a- (*R*)-**5**, **-9**, 12-(*S*)-**5**, **-9** and 14a- (*R*)-**12**. Supplementary data associated with this article can be found in the online version, at doi:10.1016/j.tet.2010.08.054. These data include MOL files and InChIKeys of the most important compounds described in this article.

References and notes

1. (a) Terech, P.; Weiss, R. G. *Molecular Gels: Materials with Self-Assembled Fibrillar Networks*; Springer: Dordrecht, The Netherlands, 2006; (b) Smith, D. K. In *Organic Nanostructures*; Atwood, J. L., Steed, J. W., Eds.; Wiley-VCH: Weinheim, Germany, 2008; pp 111–154; (c) Prasanthkumar, S.; Saeki, A.; Seki, S.; Ajayaghosh, A. *J. Am. Chem. Soc.* **2010**, *132*, 8866–8867; (d) Sangeetha, N. M.; Maitra, U. *Chem. Soc. Rev.* **2005**, *34*, 821–836; (e) Maiti, D. K.; Halder, S.; Pandit, P.; Chatterjee, N.; De Joarder, D.; Pramanik, N.; Saima, Y.; Patra, A.; Maiti, P. K. *J. Org. Chem.* **2009**, *74*, 8086–8097; (f) Hahma, A.; Bhat, S.; Leivo, K.; Linnanto, J.; Lahtinen, M.; Rissanen, K. *New J. Chem.* **2008**, *32*, 1438–1448; (g) de Loos, M.; van Esch, J. H.; Kellong, R. M.; Feringa, B. L. *Tetrahedron* **2007**, *63*, 7285–7301; (h) Bhat, S.; Maitra, U. *Tetrahedron* **2007**, *63*, 7309–7320; (i) Pal, A.; Ghosh, Y. K.; Bhattacharya, S. *Tetrahedron* **2007**, *63*, 7334–7348; (j) Yabuuchi, K.; Tochigi, Y.; Mizoshita, N.; Hanabusa, K.; Kato, T. *Tetrahedron* **2007**, *63*, 7358–7365; (k) Huang, X.; Weiss, R. G. *Tetrahedron* **2007**, *63*, 7375–7385; (l) Wang, G.-X.; Chow, H.-F. *Tetrahedron* **2007**, *63*, 7407–7418; (m) Džolic, Z.; Cametti, M.; Cort, A. D.; Mandolini, L.; Žinić, M. *Chem. Commun.* **2007**, 3535–3537; (n) Yagai, S.; Iwashima, T.; Kishikawa, K.; Nakahara, S.; Karatsu, T.; Kitamura, A. *Chem.—Eur. J.* **2006**, *12*, 3984–3994; (o) Su, L.; Bao, C.; Lu, R.; Chen, Y.; Xu, T.; Song, D.; Tan, C.; Shi, T.; Zhao, Y. *Org. Biomol. Chem.* **2006**, *4*, 2591–2594; (p) Shirakawa, M.; Kawano, S.-i.; Fujita, N.; Sada, K.; Shinkai, S. *J. Org. Chem.* **2003**, *68*, 5037–5044; (q) Sugiyasu, K.; Fujita, N.; Takeuchi, M.; Yamada, S. *Org. Biomol. Chem.* **2003**, *1*, 895–899; (r) Jung, J. H.; Shinkai, S. *J. Chem. Soc., Perkin Trans. 2* **2000**, 2393–2398; (s) Hafkamp, R. J. H.; Feiters, M. C.; Nolte, R. J. M. *J. Org. Chem.* **1994**, *64*, 412–426.
2. (a) Sugiyasu, K.; Fujita, N.; Shinkai, S. *Angew. Chem., Int. Ed.* **2004**, *43*, 1229–1233; (b) Ajayaghosh, A.; Praveen, V. K.; Vijayakumar, C. *Chem. Soc. Rev.* **2008**, *37*, 109–122; (c) Kubo, W.; Murakoshi, K.; Kitamura, T.; Wada, Y.; Hanabusa, K.; Shirai, H.; Yanagida, S. *Chem. Lett.* **1998**, 1241–1242; (d) Sone, E. D.; Zubarev, E. R.; Stupp, S. I. *Angew. Chem., Int. Ed.* **2002**, *41*, 1705–1709; (e) Ajayaghosh, A.; Praveen, V. K. *Acc. Chem. Res.* **2007**, *40*, 644–656; (f) Roubeau, O.; Colin, A.; Schmitt, V.; Clerac, R. *Angew. Chem., Int. Ed.* **2004**, *43*, 3283–3286; (g) Ayabe, M.; Kishida, T.; Fujita, N.; Shinkai, S. *Org. Biomol. Chem.* **2003**, *12*, 2744–2747; (h) Niesz, K.; Yang, P.; Somorjai, G. A. *Chem. Commun.* **2005**, 1986–1987; (i) Ono, Y.; Nakashima, K.; Sano, M.; Kanekiyo, Y.; Inoue, K.; Hojo, J.; Shinkai, S. *Chem. Commun.* **1998**, 1477–1478; (j) van Bommel, K. J. C.; Friggeri, A.; Shinkai, S. *Angew. Chem., Int. Ed.* **2003**, *42*, 980–999; (k) Sugiyasu, K.; Fujita, N.; Shinkai, S. *J. Mater. Chem.* **2005**, *15*, 2747–2754; (l) Alvord, L.; Court, J.; Davis, T.; Morgan, C. F.; Schindhelm, K.; Vogt, J.; Winterlon, L. *Optom. Vis. Sci.* **1998**, *75*, 30–36; (m) Berger-Galley, C.; Latouche, X.; Illouz, Y. G. *Aesthetic Plast. Surg.* **2001**, *25*, 249–255; (n) Estroff, L. A.; Addadi, L.; Weiner, S.; Hamelton, A. D. *Org. Biomol. Chem.* **2004**, *2*, 137–141.
3. (a) van Esch, H.; de Feyter, S.; Kellogg, R. M.; de Schryver, F.; Feringa, B. L. *Chem.—Eur. J.* **1997**, *3*, 1238–1243; (b) Schoonbeek, F. S.; van Esch, J. H.; Wesewijs, B.; Rep, D. B. A.; de Haas, M. P.; Klapwojk, T. M.; Kellog, R. M.; Feringa, B. L. *Angew. Chem., Int. Ed.* **1999**, *38*, 1393–1397; (c) Sessler, J. L.; Jayawickramarajah, J. *Chem. Commun.* **2005**, 1939–1949.
4. (a) Desiraju, G. R. *Crystal Engineering: The Design of Organic Solids*; Elsevier: Amsterdam, 1989; (b) Hunter, C. A. *Chem. Soc. Rev.* **1994**, *23*, 101–109; (c) Desiraju, G. R. *Curr. Sci.* **2001**, *81*, 1038–1042; (d) Burley, S. K.; Petsko, G. A. *Science* **1985**, *229*, 23–28; (e) Brammer, L. *Chem. Soc. Rev.* **2004**, *33*, 476–489.
5. (a) Schweizer, E. E.; Nyez-Meeder, O. In *The Chemistry of Heterocyclic Compounds*; Ellis, G. P., Ed.; Wiley-Interscience: New York, 1977; Vol. 31, pp 11–139; (b) Bowers, S.; Ohta, T.; Cleere, J.-S.; Marsella, P. A. *Science* **1976**, *193*, 542–547.
6. Booma, C.; Balasubramanian, K. K. *Tetrahedron Lett.* **1993**, *34*, 6757–6760.
7. (a) Ramesh, N. G.; Balasubramanian, K. K. *Eur. J. Org. Chem.* **2003**, *68*, 4477–4487; (b) Ghosh, R.; Chakraborty, A.; Maiti, D. K.; Puranik, V. G. *Tetrahedron Lett.* **2005**, *46*, 8047–8051; (c) Ghosh, R.; Chakraborty, A.; Maiti, D. K.; Puranik, V. G. *Org. Lett.* **2006**, *8*, 1061–1064; (d) Santhi, M.; Balasubramanian, K. K.; Bhagavathy, S. *Carbohydr. Res.* **2009**, *344*, 521–525.
8. (a) Yan, M. C.; Jang, Y. J.; Yao, C. F. *Tetrahedron Lett.* **2001**, *42*, 2717–2721; (b) Bachman, B.; Levine, H. A. *J. Am. Chem. Soc.* **1948**, *70*, 599–601; (c) Dauzonne, D.; Rene, R. *Synthesis* **1984**, 348–349; (d) Bandyopadhyay, C.; Sur, K. R. *Indian J. Chem.* **2000**, *39B*, 137–140; (e) Sosnovskikh, V. Y.; Korotaev, V. Y.; Chizhov, D. L.; Kutyashev, I. B.; Yachevskii, D. S.; Kazheva, O. N.; Dyachenko, O. A.; Charushin, V. N. *J. Org. Chem.* **2006**, *71*, 4538–4543.
9. Yadav, J. S.; Reddy, B. V. S.; Aruna, M.; Venugopal, C.; Ramalingam, T.; Kumar, S. K.; Kunwar, A. C. *J. Chem. Soc., Perkin Trans. 1* **2002**, 165–171.

10. (a) Ghosh, R.; De, D.; Shown, B.; Maiti, S. B. *Carbohydr. Res.* **1999**, *321*, 1–3; (b) Ghosh, R.; Chakraborty, A.; Maiti, D. K. *Synth. Commun.* **2003**, *33*, 1623–1632; (c) Ghosh, R.; Chakraborty, A.; Maiti, S. *Arkivoc* **2004**, *xiv*, 1–9; (d) Dassarma, M.; Ghosh, R.; Patra, A.; Chowdhury, R.; Chaudhuri, K.; Hazra, B. *Org. Biomol. Chem.* **2007**, *5*, 3115–3125; (e) Roy, S.; Chakraborty, A.; Ghosh, R. *Carbohydr. Res.* **2008**, *343*, 2523–2529; (f) Maity, S. K.; Maity, S.; Patra, A.; Ghosh, R. *Tetrahedron Lett.* **2008**, *49*, 5847–5849; (g) Maity, S. K.; Patra, A.; Ghosh, R. *Tetrahedron* **2010**, *66*, 2809–2814.
11. (a) Turro, N. J. *Modern Molecular Photochemistry*; University Science Books: 1991; (b) Birks, J. B. *Rep. Prog. Phys.* **1975**, *38*, 903–974; (c) Birks, J. B. *Photophysics of Aromatic Molecules*; Wiley-Interscience: 1970.
12. (a) An, B. K.; Kwon, S. K.; Jung, S. D.; Park, S. Y. *J. Am. Chem. Soc.* **2002**, *124*, 14410–14415; (b) An, B. K.; Lee, D. S.; Lee, J. S.; Park, Y. S.; Song, H. S.; Park, S. Y. *J. Am. Chem. Soc.* **2004**, *126*, 10232–10233.
13. (a) Andrieux, K.; Lesieur, P.; Lesieur, S.; Ollivon, M.; Grabielle-Madelmont, C. *Anal. Chem.* **2002**, *74*, 5217–5226; (b) Xiao, S.; Zou, Y.; Yu, M.; Yi, T.; Zhou, Y.; Li, F.; Huang, C. *Chem. Commun.* **2007**, 4758–4760.
14. (a) Tata, M.; John, V. T.; Waguespack, Y. Y.; McPherson, G. L. *J. Phys. Chem.* **1994**, *98*, 3809–3817; (b) Jung, J. H.; Shinkai, S.; Shimizu, T. *Chem.—Eur. J.* **2002**, *8*, 2684–2690.
15. (a) Feng, Y.; Liu, Z.-T.; Liu, J.; He, Y.-M.; Zheng, Q.-Y.; Fan, Q.-H. *J. Am. Chem. Soc.* **2009**, *131*, 7950–7951; (b) Ajayaghosh, A.; George, S. J. *J. Am. Chem. Soc.* **2001**, *123*, 5148–5149.
16. CCDC-766341 [for 10a-(*R*)-**10**] contains the supplementary crystallographic data. These data can be obtained free of charges from The Cambridge Crystallographic Data Centre via www.ccdc.cam.ac.uk/data_request/cif.
17. Altomare, A.; Giacovazzo, C.; Guagliardi, A.; Moliterni, A. G. G.; Rizzi, R.; Werner, P. E. *J. Appl. Crystallogr.* **2000**, *33*, 1180–1186.
18. Favre-Nicolin, V.; Cerny, R. *J. Appl. Crystallogr.* **2002**, *35*, 734–743; http://objcryst.sourceforge.net.
19. Stewart, J. J. *J. Mol. Model* **2007**, *13*, 1173–1213.
20. Larson, A. C.; Von Dreele, R. B. In General Structure Analysis System (GSAS), Los Alamos National Laboratory Report LAUR 86-748, 2000.